Fast soft x-ray images of magnetohydrodynamic phenomena in NSTX[a)]

C. E. Bush,[1,b)] B. C. Stratton,[2,c)] J. Robinson,[2] L. E. Zakharov,[2] E. D. Fredrickson,[2] D. Stutman,[3] and K. Tritz[3,d)]
[1]*Oak Ridge National Laboratory, Oak Ridge, Tennessee 37831, USA*
[2]*Princeton Plasma Physics Laboratory, Princeton, New Jersey 08543, USA*
[3]*Johns Hopkins University, Baltimore, Maryland 21218, USA*

(Presented 13 May 2008; received 22 May 2008; accepted 17 July 2008; published online 31 October 2008)

A variety of magnetohydrodynamic (MHD) phenomena have been observed on NSTX. Many of these affect fast particle losses, which are of major concern for future burning plasma experiments. Usual diagnostics for studying these phenomena are arrays of Mirnov coils for magnetic oscillations and *p-i-n* diode arrays for soft x-ray emission from the plasma core. Data reported here are from a unique fast soft x-ray imaging camera (FSXIC) with a wide-angle (pinhole) tangential view of the entire plasma minor cross section. The camera provides a 64×64 pixel image, on a charge coupled device chip, of light resulting from conversion of soft x rays incident on a phosphor to the visible. We have acquired plasma images at frame rates of 1–500 kHz (300 frames/shot) and have observed a variety of MHD phenomena: disruptions, sawteeth, fishbones, tearing modes, and edge localized modes (ELMs). New data including modes with frequency >90 kHz are also presented. Data analysis and modeling techniques used to interpret the FSXIC data are described and compared, and FSXIC results are compared to Mirnov and *p-i-n* diode array results. © *2008 American Institute of Physics.* [DOI: 10.1063/1.2968219]

I. INTRODUCTION

The fast soft x-ray (SXR) imaging camera (FSXIC) is now established as a major diagnostic for study of magnetohydrodynamic (MHD) instabilities in high temperature magnetically confined plasmas. It has now been used for MHD studies on several toroidal fusion research devices. These include the Tokamak Experiment for Technology Oriented Research (TEXTOR), the Large Helical Device (LHD), and the National Spherical Torus Experiment (NSTX) at the Princeton Plasma Physics Laboratory. Theory indicates that the alpha heating power in sawtoothing ITER discharges could be reduced compared to nonsawtoothing plasmas. Effects on alphas have been observed experimentally during sawtoothing deuterium-tritium (DT) discharges on TFTR and JET. Theory and experiment also indicate that sawteeth cause redistribution of fast particles resulting from neutral beam injection (NBI). It is important for STs, ITER, and ITPA database aspect ratio scaling to understand the spatial structure of the associated modes in order to understand how they interact with the fast particles. We have studied the spatial structure and time behavior of the MHD in NSTX using fast SXR camera imaging. This includes use of a range of Be foil thicknesses to investigate different parts of the SXR spectra emitted from the high temperature NSTX plasma, much of which may be associated with different MHD modes. Highly reproducible and strongly sawtoothing target plasmas are also used. One example was a 1 s duration discharge, which showed energetic particle mode (EPMs) early in the shot and later, sawteeth, when the q was reduced. In addition it is possible the sawteeth could trigger neoclassical tearing mode (NTMs). The target discharges include *L*-mode, *H*-mode, and He plasmas.

The goal is to study the physics of the interaction of the MHD with the plasma on NSTX using fast SXR camera imaging. We have acquired plasma images at frame rates of 1–500 kHz and have observed a variety of MHD phenomena: internal reconnection events, disruptions, sawteeth, fishbones, tearing modes, and ELMs. This is important to ITER due to fast particle (α's, etc.) losses.

II. EXPERIMENTAL SETUP

The pinhole camera with a wide-angle tangential view of the plasma[1–4] is based on the Princeton Scientific Instruments PSI-5 charge coupled device (CCD) camera. It has a 64×64 pixel image and frame rates up to 500 kHz for 300 frames. The SXRs ($\sim$1–5 keV) are converted to visible light by fast P47 phosphor deposited on a fiber-optic faceplate, and an electrostatic image intensifier and lenses demagnify the image by 6:1 and couple visible light to the CCD. The size (1–5 mm diameter) of the pinhole can be changed from a remote location (remotely selectable), in the case of NSTX, the control room. This allows trade-off of spatial resolution and signal level, and the remotely selectable beryllium foils allow low-energy cutoff of the SXRs

[a)]Contributed paper, published as part of the Proceedings of the 17th Topical Conference on High-Temperature Plasma Diagnostics, Albuquerque, New Mexico, May 2008.
[b)]Electronic mail: bush@pppl.gov.
[c)]Electronic mail: bstratton@pppl.gov.
[d)]Electronic mail: ktritz@pppl.gov.

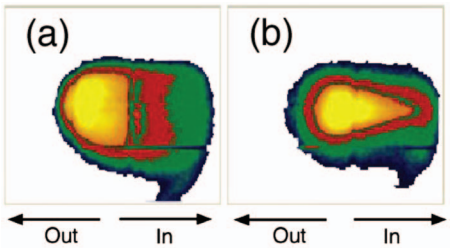

FIG. 1. (Color) FSXIC image for one frame of the 300 recorded for shot 113778.

incident on the phosphor to be varied. The horizontal field of view of the FSXIC includes nearly the full minor cross section of the NSTX chamber.

In NSTX, β_t is normally relatively high such that the hot core is Shafranov shifted toward the low B_t field side of the cross section that is always fully viewed by the FSXIC. This cross section is viewed through a pinhole, which is essentially the entrance of the x rays to the camera system. Behind the pinhole is the filter array, which includes a remotely selectable array of foils with a variety of thicknesses and material (Be, Ti). The variety of filters and apertures allow viewing of a wide spectrum of plasma temperatures and MHD behavior. Much of the data to date has been obtained using the thinner Be foils, mainly a 7.6 μm Be foil, thus limiting observation to lower temperature (often Ohmic) plasmas. In many cases coherent modes and their time behavior and spatial extent are clearly discernable in the images before additional processing.

III. RESULTS AND DISCUSSION

A good example illustrating the effectiveness of images (or snapshots) of MHD activity is that of discharge (shot) 113778. Two images for 113778 at $t=0.176$ s of the recorded 300 frames (images) taken are shown in Fig. 1. In each image, low intensity is represented by dark shades or colors and high intensity by light colors to a maximum represented by white. The two images are representative of the extremes of the first half of each cycle of the mode. A half cycle begins with Fig. 1(a) and ends with Fig. 1(b), in both of which the highest intensity region is centered about the midplane. A movie of the 300 images shows the high intensity spot to begin shifting downward. This continues for a few frames, then the high intensity spot shifts to the right, and then upward until it again reaches the midplane where it has acquired the shape of the image in Fig. 1(b). Then for the second half, the high intensity spot shifts upward, to the left, and down as it progresses back to Fig. 1(a). Thus the train of 300 frames, i.e., 64×64 pixel images/snapshots shows the time evolution of the mode structure.

In this case the dynamics of the images correlated very well with data from core chordal data of an array of SXR diodes. Figure 2 shows time traces for a centrally viewing and two off axis viewing SXR diodes. The SXR diodes show the mode to turn on at $t=0.1735$ s and oscillate at 2.5 kHz through the time of Fig. 2. The camera was run at 100 kHz (10 μs/frame) for 3 ms beginning at $t=0.175$ s, missing the first two or three cycles, and ending at $t=0.178$ s.

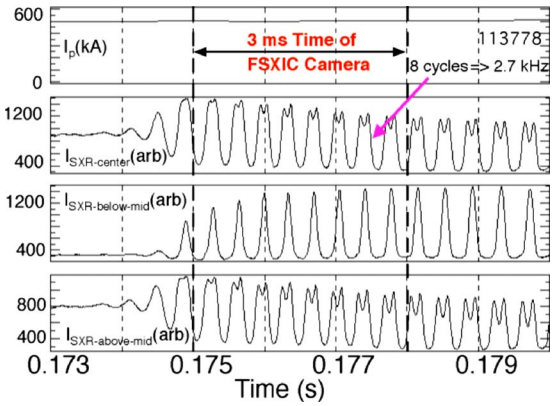

FIG. 2. (Color online) Ip and three SXR diode time traces for shot 113778. The first is for a centrally viewing diode, the second is for a diode viewing below, and the third for a diode viewing above the midplane.

The $m/n=1/1$ tearing mode of Fig. 2 observed using the FSXIC images, showed structure with coherent oscillations. This was in agreement with the (central) chords of the SXR array data plotted in Fig. 2. The plasma current was $I_p=500$ kA. The effects of the mode were seen in the stored energy, which decreased rapidly at the onset of the mode at $t=0.174$ s. A singular value decomposition (SVD) analysis was done of the full train of images,[5] 300 frames, from $t=175$ s to $t=0.178$ s. The SVD was used in order to extract separate coherent fluctuations in space and time from background noise. SVD analysis identifies major components of the dynamics recorded in the images. The camera images yield a matrix $A(M\times N)$ of N time series of M frames, where $M=300$ frames per shot. The matrix A is decomposed into three matrices such that

$$A(\mathrm{MxN}) = \mathrm{UWV}^T,$$

where $U(M\times N)$—columns are spatial vectors (topos)—and $V(N\times N)$—columns are temporal vectors (chronos) and $W(N\times N)$ a diagonal matrix (of weights).

Figure 3 summarizes results of the SVD, Figs. 3(a)–3(k), where Figs. 3(b)–3(f) are the time (chronos, V0–V4) behaviors of the first five dominant modes and Figs. 3(g)–3(k) are the respective spatial structures (topos, U0–U4) for each of

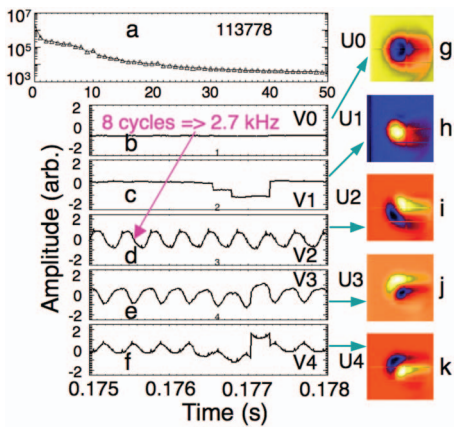

FIG. 3. (Color) Results of SVD for shot 113778.

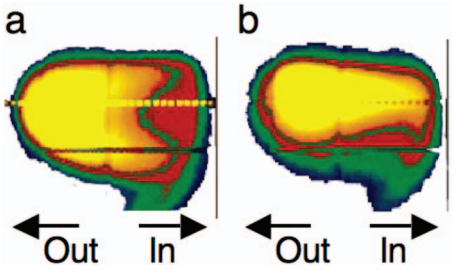

FIG. 4. (Color) Two consecutive (in time) FSXIC frames for shot 113355.

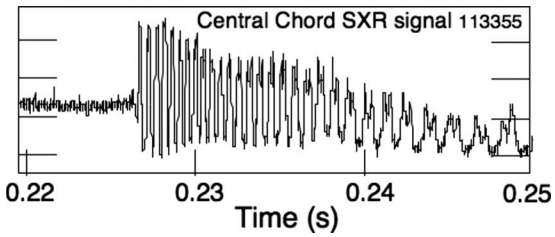

FIG. 5. SXR diode trace for shot 113355.

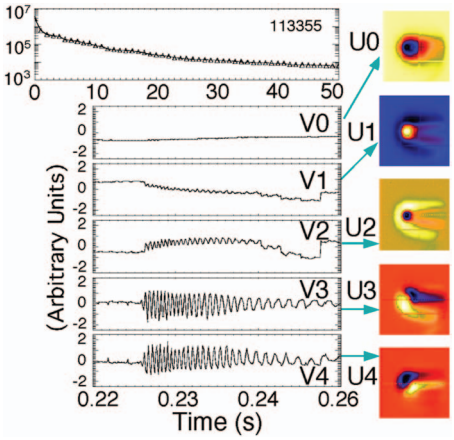

FIG. 6. (Color) SVD for shot 113355. The chronos match the time behavior of the SXR diode of Fig. 5.

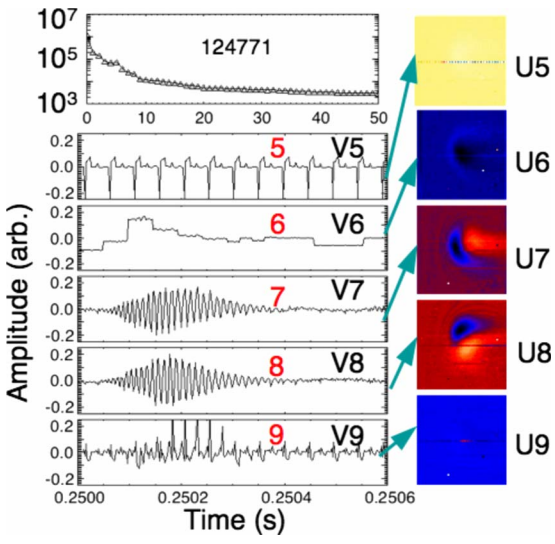

FIG. 7. (Color online) SVD for a shot (124771) for which the FSXIC showed a high frequency, 90 kHz, $n=3$ MHD mode.

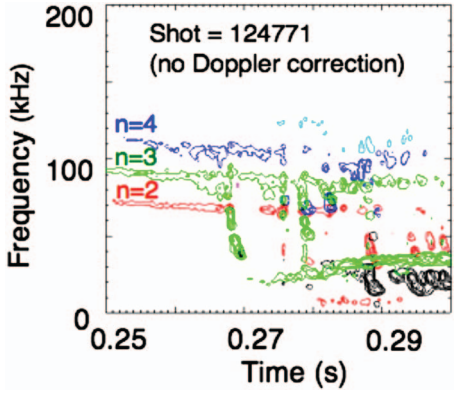

FIG. 8. (Color) Time resolved spectra of magnetic fluctuations from arrays of Mirnov coils. Clearly indicated is the existence of $n=3$ fluctuations at 90 kHz at the same time of the modes with the same frequency indicated in the SVD analysis of Fig. 7.

the chronos. Note that the oscillations in Figs. 3(d) and 3(e) match up exactly with the same time of the oscillations in the SXR traces of Fig. 2.

Figure 4 shows two frames of a second plasma that were taken 2 ms apart. A centrally viewing (perpendicular) SXR diode trace for the plasma is shown in Fig. 5. The MHD mode is triggered at $t=0.226$ s, beginning at a modest oscillation frequency and slows to a lower frequency toward the end of the burst. In this case the FSXIC was operated at 10 kHz, so that the 300 frames covered 30 ms or nearly the full duration of the MHD burst. Again a SVD analysis of the images was done and the results are shown in Fig. 6 (shot 113355). The chronos V3 and V4, extracted by the SVD clearly match the SXR diode time trace of Fig. 5. Some of the major topos are slightly more complex in this case than those for the case of Fig. 3.

The results for a third and final example are given in Figs. 7 and 8. The main difference for this case was that the camera was run at 500 kHz and therefore was able to capture higher frequency MHD phenomena. In this case the 300 frames were acquired at 2 μs/frame for 0.6 ms of the discharge beginning at 0.2500 s and ending at 0.2506 s. The oscillations were very clear and detailed in the movie of the 300 images, beginning with a quiescent frame to frame behavior then showing triggering of a mode having a high frequency, growing in amplitude while gradually slowing, peaking, and then slowly decreasing in amplitude and disappearing, all during the 300 frames (0.6 ms). This activity is shown quantitatively in the SVD results given in Fig. 8. A main difference in SVD results for the third example from the first two is that no coherent modes were found in the first five chronos, but only in the second five V7 and V8, respectivley. From the SVD it was determined that the mode frequency was ~90 kHz, and this result is to be compared to the magnetic data described in the next paragraph.

Figure 8 shows results from analysis of data from Mirnov coil arrays and is a plot of the spectra of magnetic fluctuations versus time. The FSXIC data were taken within 0.6 ms of the beginning of the plot at 0.25 s. The frequency data are plotted from 0.25 to 0.30 s. The Mirnov data show coherent activity at three MHD mode values, $n=2$, 3, and 4

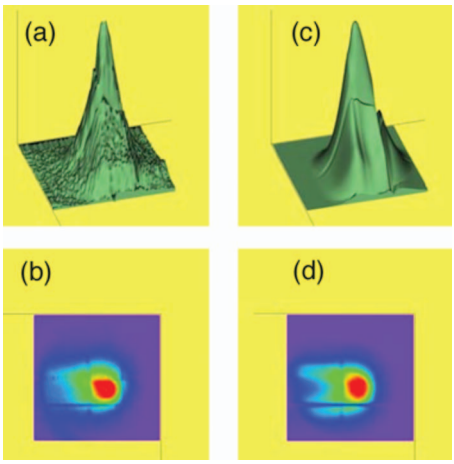

FIG. 9. (Color) (a) Surface and (b) contour plots of actual plasma emissivity (from FSXIC images) for shot 113355. The reconstructions are shown in (c) and (d), respectively.

at 70, 90, and 110 kHz, respectively, during the first 10 ms of the plot. The $n=3$ mode agrees with the 90 kHz mode given by the SVD analysis of the train of FSXIC images.

A code (CBBST) (Ref. 6) was written to simulate the line integral of the camera data and to invert it assuming a simple spatial dependence of $\varepsilon=\varepsilon(a+\hat{\imath})$, where a is a flux surface label corresponding to the square root of the toroidal magnetic flux and $\hat{\imath}(a,\theta,\phi)$ is a perturbation that may include both ideal and tearing types of perturbations. Steplike $m/n=1/1$ perturbations were considered. For this report a simulation was done for the example plasma of Figs. 4–6, however the technique is also applicable to the other two plasma examples. The results of the simulation are given in Fig. 9.

The 21 radial values of the ε (a_i) function and the amplitude and phase of the $\hat{\imath}_{1/1}$ perturbation are reconstructed from the 64×64 data array S_{ij} using SVD and an iterative technique for solving the integral equation, which becomes nonlinear in the presence of perturbations. The plasma equilibrium was generated by the Equilibrium and Stability Code[4] using a plasma boundary reconstructed by the EFIT code and TRANSP code simulations of plasma pressure and q profiles. It is clear that the results of the simulation, Figs 9(c) and 9(d) agree well with the surface, Fig. 9(a), and contour, Fig. 9(b), plots of the experimental FSXIC data.

IV. CONCLUSIONS

A variety of MHD cases have been investigated on NSTX using the FSXIC. Three cases were presented and discussed in this report. The possible existence of MHD modes was indicated simply by viewing movies made from FSXIC images. Simple $m/n=1/1$ modes were clear in the camera images and in results of SVD analysis. An $n=3$ mode determined from the combination of SVD analysis of FSXIC images and magnetic fluctuation data was shown. Results for operation of the camera at three framing rates, 10, 100, and 500 kHz, showed MHD modes at frequencies from a low of 2 kHz to a high of 90 kHz. SVD analysis was effective in determining mode frequencies and spatial structure. These were found to agree with or compliment results from SXR array and Mirnov coil array data.

ACKNOWLEDGMENTS

The authors would like to give special thanks to Doug Labrie of the NSTX team of PPPL and Vince Mastrocola of Princeton Scientific Instruments. We also thank Dr. Satoshi Ohdachi for providing the software for carrying out the SVD analyses. This work was supported by U.S. DOE Contract No. DE-AC05–00OR22725.

[1] S. von Goeler, R. Kaita, M. Bitter, G. Fuchs, M. Poier, G. Bertschinger, H. R. Kosloski, K. Toi, S. Ohdachi, and A. Donne, Rev. Sci. Instrum. **70**, 599 (1999).
[2] B. C. Stratton, R. Feder, S. von Goeler, G. F. Renda, V. J. Mastrocola, and J. L. Lowrance, Rev. Sci. Instrum. **75**, 3959 (2004).
[3] B. C. Stratton, S. von Goeler, D. Stutman, K. Tritz, and L. E. Zakharov, 32nd EPS Conference on Plasma Physics, Tarragona, Spain, 27 June–1 July 2005 (ECA, 2005), Vol. 29C, p. 1.060.
[4] B. C. Stratton, S. von Goeler, D. Stutman, K. Tritz, and L. E. Zakharov, "Be Foil Filter Knee Imaging NSTX Plasma with Fast Soft X-Ray Camera," PPPL Report No. PPPL-4093, August 2005.
[5] S. Ohdachi, K. Toi, G. Fuchs, S. von Goeler, and S. Yamamoto, Rev. Sci. Instrum. **74**, 2136 (2003).
[6] L. E. Zakharov and A. Pletzer, Phys. Plasmas **6**, 4693 (1999).